The generation of small melt-fractions in truncated melt columns: constraints from magmas erupted above slab windows and implications for MORB genesis

MALCOLM J. HOLE

Department of Geology and Petroleum Geology, University of Aberdeen, Aberdeen, AB9 2UE, UK

AND

ANDY D. SAUNDERS

Department of Geology, University of Leicester, University Road, Leicester, LE1 7RH, UK

Abstract

At a number of locations along the Pacific margin of the Americas and west Antarctica, small volumes of alkalic basalts were erupted following successive ridge crest-trench collisions. The basalts were generated as a result of upwelling of asthenosphere through windows in the subducted plate. There is no evidence for local high temperature mantle plumes or significant lithospheric extension associated with these basalts. For the best sampled area, the Antarctic Peninsula, mean values for fractionation-corrected iron content (FeO*) vary from 6.9 to 10.6 wt.%, and for Na_2O ($Na_{8.0}$) from 3.25 to 4.6 wt.%, implying generation of small melt-fractions at variable mean pressures. The results of rare earth element inversion modelling yield a melt generation interval of 100 to 52 km, with a maximum melt fraction of *c.* 7% generated from a MORB-like source at T_p 1300°C. Trace element and isotope systematics are also consistent with the generation of the basalts from a MORB-like source.

Mean pressures of melt generation increase with increasing distance from the original trench, but trace element and $Na_{8.0}$ data suggest that there is no systematic variation in extent of melting with distance from the trench. The data are consistent with a model whereby a MORB melting column, initially intersecting the peridotite solidus at between 15 and 30 kbar, is truncated by a lithospheric cap which thickens from *c.* 15–20 km ($\approx$5–8 kbar) up to a maximum of *c.* 50 km ($\approx$ 15 kbar), such that the mean pressures of melting increase with increasing distance from the palaeo-trench. The MORB-like major element geochemistry of basalt samples closest to the ancestral trench are consistent with initial intersection of the peridotite solidus at low pressures (*c.* 15 kbar). For areas of thickest lithosphere, mean pressures of melt generation are higher, but extents of melting are lower than for a MORB melting column with a similar initial pressure of intersection of the peridotite solidus. All these basalts therefore potentially represent analogues for the small melt-fraction precursors to the generation of MOR tholeiites.

Thermal constraints suggest that these low volume, small melt-fractions, were generated with CO_2 on the solidus, because mean pressures of melt generation are greater than the pressure of intersection of the T_p 1300°C mantle adiabat and the dry peridotite solidus. Potentially, all MORB may be generated initially with CO_2 on the solidus, and if this is correct, it does not require thermal anomalies to generate large extents of melting at high mean pressures.

KEYWORDS: MORB, melting columns, Antarctic Peninsula, *REE* inversion, slab windows.

Mineralogical Magazine, February 1996, Vol. 60, pp. 173–189

Introduction

THE generation of mid-ocean ridge basalts (MORB) is considered to be a multi-stage process involving variable extents of partial melting of mantle peridotite over a broad range of pressures. The concept of a 'melt column', where melting is initiated at pressures of up to 40 kbar and ceases at the base of the oceanic lithosphere, is now well-established in the literature (McKenzie, 1984, 1985*a*; Klein and Langmuir, 1987, 1989; McKenzie and Bickle, 1988; Elliot *et al.*, 1991). The composition of MORB, distant from the influence of higher temperature mantle plumes, appears to require integration of melts generated over a range of pressures, beginning with small melt-fractions at high pressures which progressively integrate with lower pressure, higher degree melts at shallower levels. The depth at which melting is initiated was considered by Klein and Langmuir (1987) to require variability in the potential temperature of the mantle (T_p of McKenzie and Bickle 1988) because the dry peridotite solidus has a slope of *c.* 12°C kbar^{-1}.

A feature of all MORB melt columns is the production of integrated, or 'pooled' melts (e.g. Elliot *et al.*, 1991; McKenzie and Bickle, 1988). Therefore at the surface we can only sample these integrated melt compositions, and not 'instantaneous' or minimally-integrated small melt-fractions produced at the base, or near the base, of the melting column. We therefore have no direct evidence as to the composition of these small melt-fraction precursors to MOR tholeiites. Indirect evidence for their existence, however, comes from recent studies of Th-U disequilibria and the partitioning of Th and U during melting of garnet lherzolite (Beattie, 1993). These studies imply that mid-ocean ridge basalts are produced by melting of the mantle initiated at depths where garnet is stable, corroborating the theoretical melting column models for MORB generation.

Small melt-fractions can interact with lithospheric material (including earlier small melt-fractions) and undergo substantial compositional modification. Direct evidence of their composition is therefore crucial to our understanding of the evolution of isotopic diversity in the upper mantle and lithosphere. In this paper we use major element systematics, as described by Klein and Langmuir (1987, 1989) and Brodholt and Batiza (1989), and *REE* inversion modelling following the method of McKenzie and O'Nions (1991) to examine the genesis of alkalic basalts that potentially represent samples of minimally-integrated small melt-fraction precursors to MOR tholeiites. These basalts were generated as a result of ridge crest-trench collisions and formation of slab windows. We show that in this tectonic setting, a MORB melting column is progressively truncated by the overlying lithospheric cap, such that small melt-fractions are generated at high mean pressures, and the erupted compositions preserve high pressure chemistry. There is no evidence for local high temperature mantle plumes in this tectonic setting and *REE* inversion modelling indicates that for mantle with T_p = 1300°C, melting would have to take place at temperatures lower than that of the dry peridotite solidus.

Slab window formation and the geochemistry of alkalic basalts

The geochemistry and tectonic affinities of the alkalic basalts generated after slab window formation along continental margins are described in detail elsewhere (e.g. N America, Thorkelson and Taylor, 1989; San Quintìn (Baja California), Dickinson and Snyder, 1979; Saunders *et al.*, 1987; S California, Johnson and O'Neil, 1984; British Columbia, Bevier, 1983; S Chile, Forsythe and Nelson, 1985; Antarctic Peninsula, Hole, 1988, 1990; Hole and Larter 1993; Hole *et al.*, 1991, 1993, 1995). In this paper we will concentrate on one of the simplest tectonic scenarios for slab window formation and related magmatism, that of the Antarctic Peninsula.

Slab window formation along the Antarctic Peninsula

Following more than 200 m.y. of subduction of Pacific oceanic crust beneath the west coast of the Antarctic Peninsula, subduction ceased by a series of ridge crest-trench collisions. Large transform offsets had segmented the spreading axis, with the result that although the plate convergence was almost orthogonal, the southernmost ridge segments collided with the margin long before the more northerly segments. This resulted in a series of eight discrete northward-younging ridge crest-trench collisions events, starting at approximately 50 Ma in the south, with the youngest collision event occurring at ≈4 Ma in the north of the peninsula (Barker, 1982; Larter and Barker, 1991). Because the oceanic and continental lithosphere in this area were part of the same plate, a part of the continental margin was converted from a convergent to passive margin following each collision event (Barker, 1982; Larter and Barker, 1991). Throughout this period, segments of previously subducting oceanic lithosphere became detached from the spreading ridge at the continental margin, but continued to be subducted at the rate of spreading of the next ridge segment to the north. The important result was the formation of an extensive slab window complex beneath the continental lithosphere, and the eruption of alkalic basalts. The

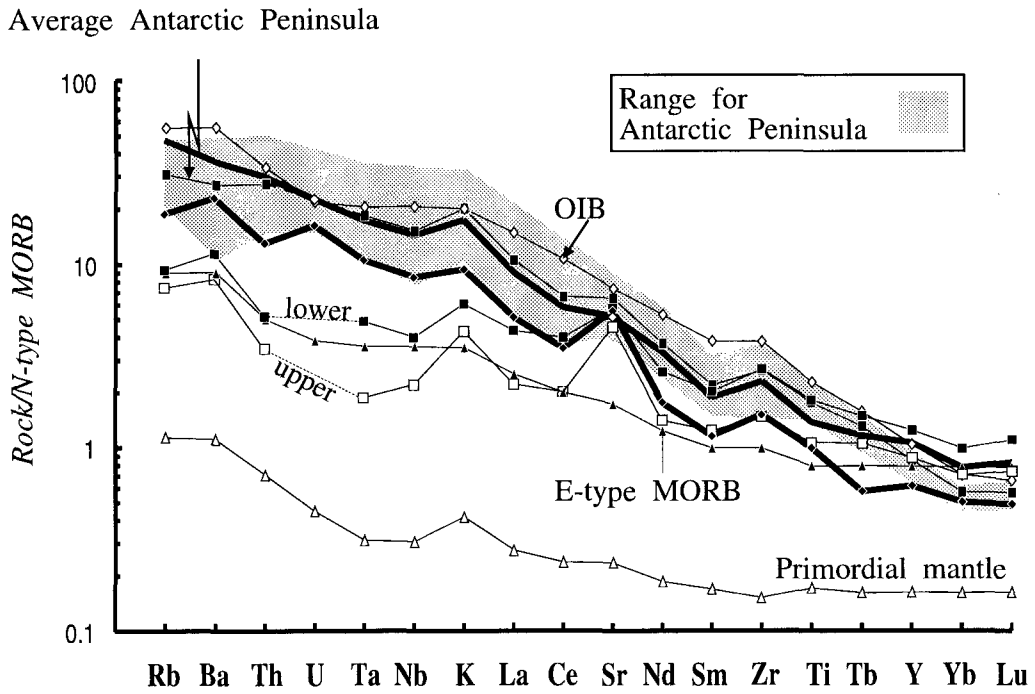

FIG. 1. MORB-normalized multi-element plot of range for, and average of, 43 slab window-related basalts from the Antarctic Peninsula (Hole, 1988, 1990; Hole *et al.*, 1993), average OIB, E-type MORB, Primordial Mantle and normalizing values from Sun and McDonough (1989). Dredge site 138 basalts are shown in heavy lines (Hole and Larter, 1993); Brabant Island upper (open squares) and lower (filled squares) (author's unpublished data, MJH 1989). Note the positive Sr spikes for the Brabant Island basalts. The average Antarctic Peninsula basalt is the same as that used in inversion modelling (see Fig. 8*a*).

passage of the subducted slab through the upper mantle to form a slab window produced an incipient void in the mantle, which was progressively filled by upwelling asthenosphere, thus giving the potential for decompression melting. Similar tectonic events also characterized British Columbia during the Miocene and N Baja California over the past 5 Ma (Thorkelson and Taylor, 1989; Dickinson and Snyder, 1979; Rogers and Saunders, 1989).

The general trace element characteristics of the Antarctic Peninsula basalts are illustrated in Fig. 1, and show similar incompatible trace element enrichment to that seen in non-DUPAL ocean island basalts (OIB) associated with hotspots. Despite the close spatial and temporal association between the post-subduction basalts and arc-related magmatism, there is little or no evidence of a subduction-related signature in the post-subduction basalts. The Rb/Nb, Th/Nb and Ba/Nb and other LILE/HFSE ratios (e.g. Figs 1 and 2), sensitive indicators of involvement of subduction components (Pearce, 1983; Saunders *et al.*, 1988), are consistently MORB-like. Furthermore, on a plot of Ba/Nb *vs.* K/Nb (Fig. 2), the slab window-related basalts are distinguished from OIB on the basis of considerably lower Ba/Nb and higher K/Ba ratios than OIB, forming a field overlapping with the composition of N-type MORB. Isotopic data are also broadly consistent with a MORB-like depleted mantle source-region for these basalts (Hole *et al.*, 1993); all analysed samples have unradiogenic Sr (ε_{Sr} −18 to −28) and radiogenic Nd (ε_{Nd} +3.7 to +6.9) and plot slightly below the MORB field, close to the field for OIB from HIMU hotspots and the LoNd array of Hart (1988) (Fig. 3). However, the slab window-related basalts are clearly distinguished from HIMU

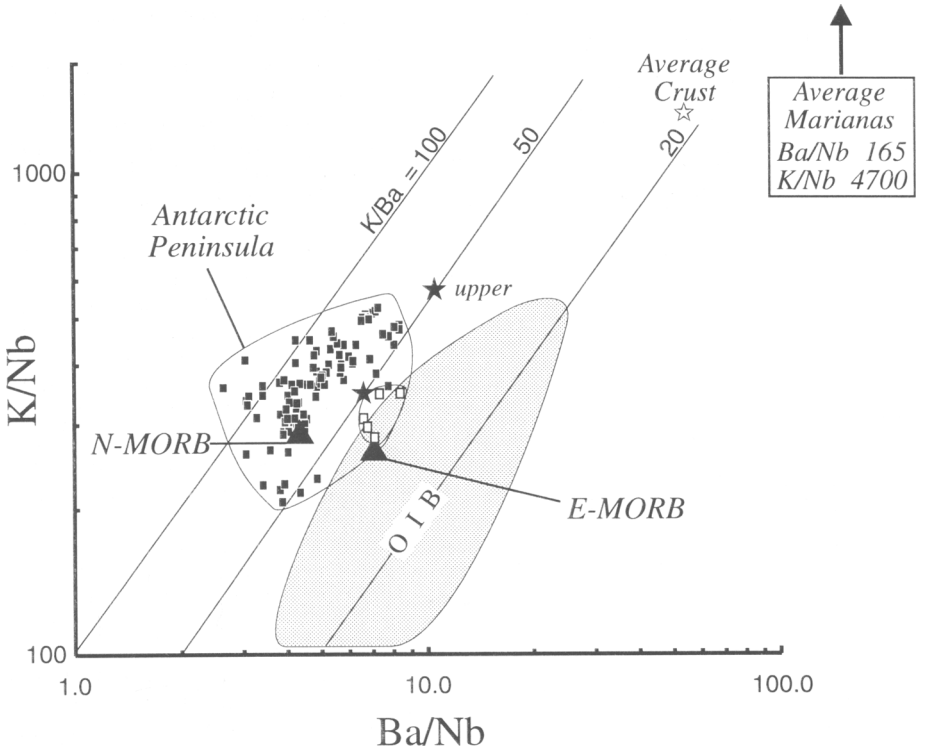

FIG. 2. Plot of Ba/Nb *vs.* K/Nb for slab window-related basalts, OIB and MORB. Note the generally higher K/Ba ratios of slab window-related basalts compared with OIB, and the lack of any trend towards continental crust or subduction-related basalts (e.g. Marianas) Data sources: OIB (Davies *et al.*, 1989; Weaver, 1991; Palacz and Saunders, 1986) Average N-MORB, E-MORB and continental crust from Sun and McDonough (1989) and Weaver (1991) Average Marianas from Hole *et al.* (1984) Symbols, filled squares, Antarctic Peninsula basalts, except open squares, dredge site 138; Brabant Island upper and lower lavas, stars.

OIB on the basis of their lower $^{206}Pb/^{204}Pb$ ratios (18.79–19.25), precluding their generation from a HIMU plume solely on geochemical grounds. For slab window-related basalts as a whole, there is no evidence for their association with significant lithospheric attenuation. Additionally, on geochemical and geological grounds, we can be confident that these basalts simply represent small degree melts of the asthenosphere unrelated to a mantle plume.

Magmagenesis

The three principle ways in which mantle melting can be initiated are: (1) adiabatic upwelling and decompression melting (e.g. at mid-ocean ridges, and during attenuation of the continental lithosphere); (2) lowering of the peridotite solidus by the addition of volatiles (e.g. at subduction zones); and (3) localized elevation of mantle temperature (hotspots). There are a number of problems in generating the Antarctic Peninsula post-subduction magmas by the above mechanisms. Firstly, there is an absence of any evidence for crustal extension, which is an effective mechanism for inducing decompression melting. Due to ice cover this is difficult to eliminate entirely in the Antarctic Peninsula, and precise figures for extension are not available, but there is no evidence for large b factors. Whilst normal faults may have enabled melt evacuation in the N Antarctic Peninsula where the eruption centres form a crudely linear array (Hole, 1990), and although this may have been sufficient to reduce the pressure on the source regions from that of a lithostatic to a fluid pressure, there is no evidence to support a model which invokes sufficient thinning of the mechanical boundary layer to induce melting (e.g. McKenzie and Bickle, 1988). Secondly, the

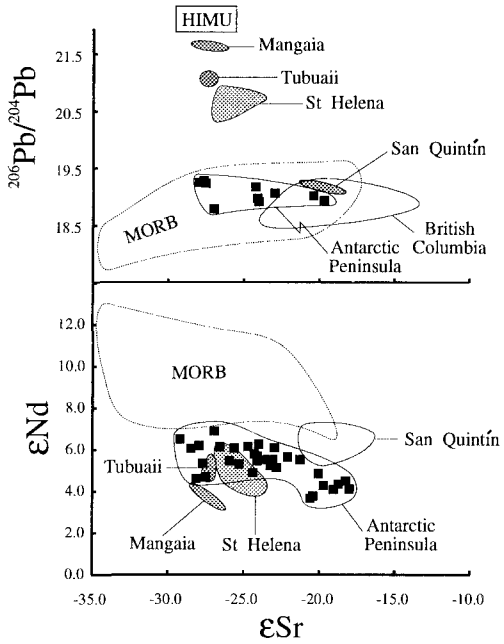

Fig. 3. Plots of εSr *vs.* εNd and $^{206}Pb/^{204}Pb$ ratios for slab window-related basalts from the Antarctic Peninsula (Hole, 1988, 1990; Hole *et al.*, 1993), British Columbia (Bevier, 1983) and San Quintín (Storey *et al.*, 1989), compared to MORB (Ito *et al.*, 1988) and HIMU OIB (Palacz and Saunders, 1986; Chaffey *et al.*, 1989; Chauvel *et al.*, 1992).

majority of the basalts show heavy *REE* (and Sc) depletion (La_n/Yb_n 6–16; Sc 13–25 ppm; Hole, 1988, 1990), indicating melting with garnet on the peridotite solidus. High-pressure melting of dry peridotite is not difficult if the mantle is sufficiently hot. Whereas many heavy *REE*-depleted continental or oceanic basalt provinces can be linked to mantle plumes, slab window-related basalts cannot because it would require elongated 'plumes' of very similar compositions to be emplaced at geographically dispersed localities, i.e. Antarctic Peninsula, Baja California and British Columbia (Thorkelson and Taylor, 1989; Hole *et al.*, 1991). Therefore, an hypothesis for asthenospheric upwelling into the incipient void formed during the opening of a slab window seems attractive. But how is melting induced? In the following sections, we utilize major element data and *REE* inversion modelling to examine the potential range of pressures and extents of melting required to generate these basalts with a view to assessing the validity of this hypothesis.

Major element data and fractionation corrections

All the major element data discussed below were analysed by XRF on fused glass discs. All iron analyses were originally reported as total iron as Fe_2O_3 and have been converted to total iron as FeO (here designated FeO*) for the purposes of fractionation correction (Klein and Langmuir, 1987). All but eight analyses of basalts from the Antarctic Peninsula were carried-out at the Department of Geology, University of Keele, UK, over an 18 month period. The data set should therefore be internally consistent. Data for Brabant Island are taken from Ringe (1991). Representative analyses of major elements for the Antarctic Peninsula basalts have been published elsewhere (Hole, 1988, 1990; Hole and Larter, 1993; Hole *et al.*, 1991, 1993, 1995) and the entire data set for the region comprises 108 analyses, the largest numbers of which are from Alexander Island and Seal Nunataks.

In investigating pressures and extents of melting, Klein and Langmuir (1987, 1989) utilized fractionation corrections for Na_2O, FeO and SiO_2 to a nominal value of MgO = 8 wt.%. The MORBs are tholeiites, and therefore exhibit early Fe enrichment on an AFM diagram, and thus the fractionation corrections for Fe to 8.0 wt.% MgO are large (e.g. DSDP Leg 407; Fig. 4*a*). The basalts under consideration here are predominantly alkali basalts and therefore do not show early Fe enrichment. The sub-horizontal arrays defined by the Antarctic Peninsula basalts on a plot of MgO *vs.* FeO*, are consistent across a very broad range of MgO contents (*c.* 5.5–12.0 wt.%; Fig. 4*a*) and therefore no correction has been applied to FeO* data (see also Brodholt and Batiza, 1987); indeed, using the correction procedure of Klein and Langmuir (1987) leads to artificially low values of $Fe_{8.0}$ (Fig. 4*a*). The Na_2O concentrations do require fractionation correction for the Antarctic Peninsula samples. However, the factors used by Klein and Langmuir (1987) again tend to over-correct the $Na_{8.0}$ content in these compositions (Fig. 4*b*), and a correction procedure (here termed $Na_{8.0}$*) more appropriate for these alkalic compositions has been calculated using data from seven lava flows of the same age from one volcanic centre in the N Antarctic Peninsula;

$$Na_{8.0}* = Na_2O + (MgO * 0.238) - 1.905 \quad (1)$$

Fractionation corrections for Na_2O were applied only to samples with 5.0–8.5 wt.% MgO. Fractionation corrections for SiO_2 are those of Klein and Langmuir (1989) for basalts in the range of 8.0–10.0 wt.% MgO. However, because at some localities there is field and geochemical evidence of localized assimilation of arkosic country rocks (Hole, 1988, 1990), major element data for samples with $^{87}Sr/^{86}Sr > 0.7031$ have not been included in the data

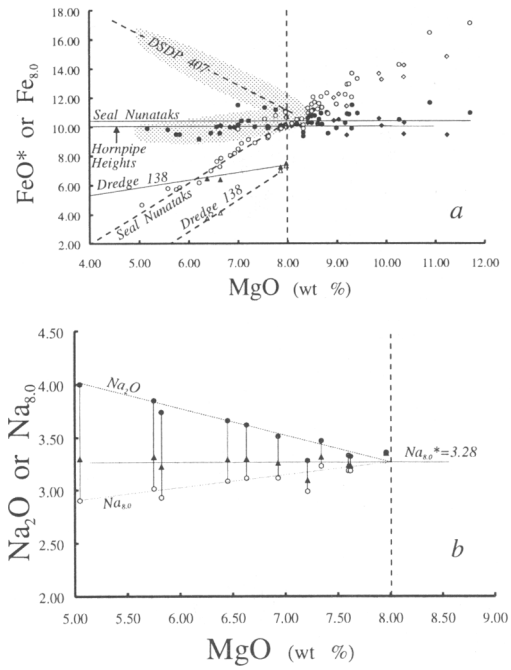

FIG. 4. (*a*) MgO versus FeO* (total iron as FeO from XRF data) and $Fe_{8.0}$ for the Antarctic Peninsula alkalic basalts. The fractionation correction of Klein and Langmuir (1987) over-corrects iron concentrations (pecked lines). The two shaded fields show the effect of fractionation correction using the method of Klein and Langmuir (1987) on MORB from DSDP Leg 49, hole 407 (Wood *et al.*, 1978). (*b*) MgO *vs.* Na_2O (dots) and fractionation corrected Na_2O ($Na_{8.0}$*; filled triangles). Open circles, fractionation correction of Klein and Langmuir (1987).

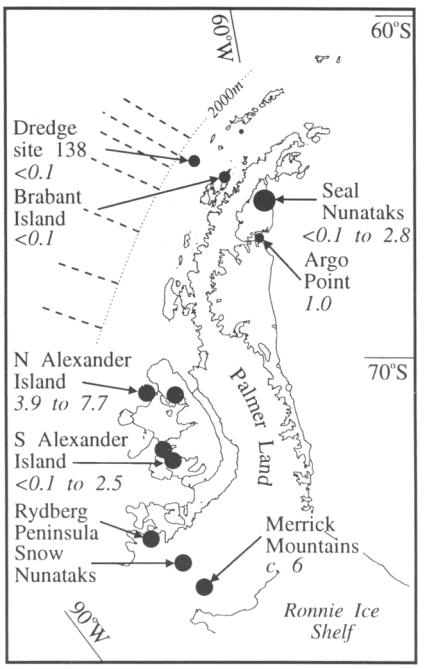

FIG. 5. Location map showing the distribution and age (in italics) of the alkalic basalts discussed in the text. Also shown are the traces of transform fracture zones (pecked lines) and the 2000 m bathymetric contour. Geochronological data from Smellie *et al.* (1988).

set. This results in the reduction of the set to 91 analyses, 76 of which fall in the range of MgO values for fractionation correction of Na_2O and 66 for SiO_2. Data have been grouped according to the geographical locations of eruptive centres (Fig. 5), which broadly correlates with age, the oldest samples being present in the areas of the older ridge crest-trench collision episodes.

Figure 6 shows FeO* and $Si_{8.0}$ *vs.* $Na_{8.0}$*. The total range of $Na_{8.0}$* is 2.8–5.0 which extends to considerably higher values than the regionally-averaged MORB data (*c.* 1.5–3.5) reported by Klein and Langmuir (1989). FeO* (Fig. 6*a*) varies from *c.* 6.4–11.4 for the Antarctic Peninsula data, the dredge site 138 samples have the lowest FeO* values (6.4–7.5) and the Brabant Island samples (note that only average major element data have been quoted in Ringe, 1991), plotting in a position intermediate between the dredge samples and Seal Nunataks. For the area that has the best sample coverage, Seal Nunataks, the data show a broad positive correlation between FeO* and $Na_{8.0}$*, overlapping with data from Snow Nunataks, a correlation that is extended by samples from S Alexander Island.

The total range of $Si_{8.0}$ is 44.5–51.7, (Fig. 6*b*) extending to lower values than regionally-averaged MORB data ($Si_{8.0}$ 48.0–52.5; Klein and Langmuir, 1989). However, because of the different MgO range for fractionation correction of SiO_2, some localities represented in Fig. 6*a* are missing from Fig. 6*b*. Data from Seal Nunataks and N Alexander Island exhibit a broad negative correlation between $Si_{8.0}$ and $Na_{8.0}$*, and in general there is an overall negative correlation between these two parameters for the entire data set. CaO/Al_2O_3 ratios vary from 0.43–0.62 considerably lower than the 0.60–0.90 range for regionally averaged MORB.

Pressure and extent of melting

Klein and Langmuir (1987) demonstrated that during partial melting of mantle peridotite, $Na_{8.0}$ decreases

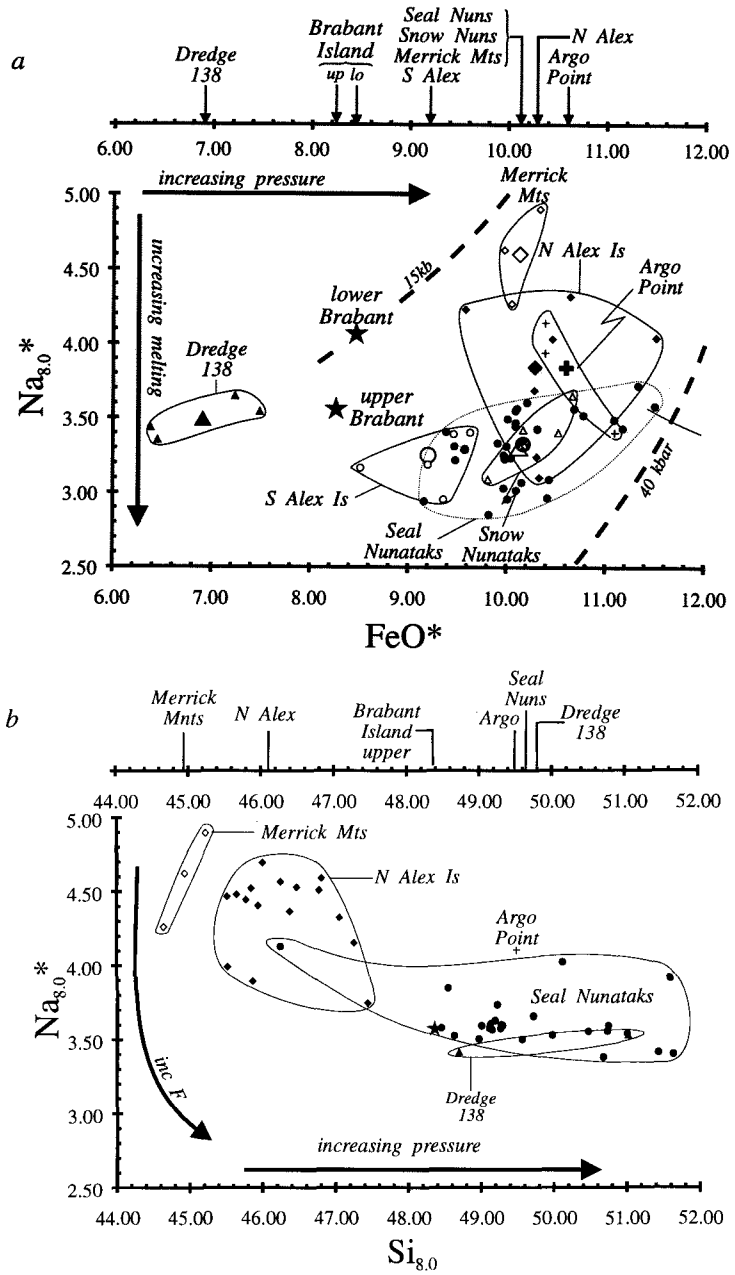

FIG. 6. Plots of (*a*) $Na_{8.0}$* *vs.* FeO* and (*b*) $Na_{8.0}$* *vs.* $Si_{8.0}$ for basalts from the Antarctic Peninsula. The two hatched lines in (*a*) are the trends for intra-column integrated melts for P_0 of 15 and 40 kbar respectively (Klein and Langmuir, 1987) Filled triangles, dredge 138; open circles, S Alexander Island; dots, Seal Nunataks; open diamonds, Merrick Mountains (LeMasurier and Thomson, 1990); crosses, Argo Point; open triangles, Snow Nunataks; filled diamonds, N. Alexander Island. Means of data are shown by the larger symbols except; Seal Nunataks, star in a circle; averages of Brabant Island lower and upper lava series, filled stars (data from Ringe, 1991). Mean FeO* and $Si_{8.0}$ for each location are plotted along the upper axes.

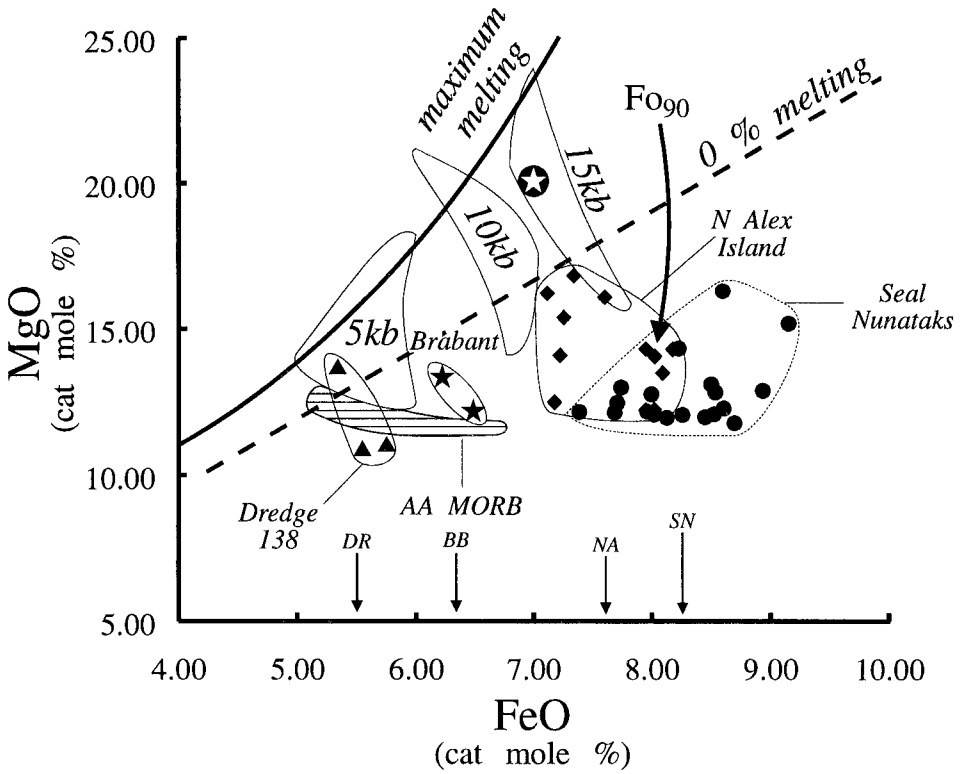

FIG. 7. Cation mole % FeO and MgO for basalts from the Antarctic Peninsula with > 9.0 wt.% MgO. Mean FeO values are plotted on the bottom axis. The heavy arrow is the fractional crystallization trajectory for olivine (Fo_{90}) The three unshaded fields represent trends for experimental melting of pyrolite at 5, 10 and 15 kbar, and the hatched field is for MORB from the Antarctic–Australia discordance (low *P* melting), after Klein and Langmuir (1987). Symbols as for Fig. 6 except star in a circle, calculated major element composition from the results of *REE* inversion.

with increasing extent of melting but is not sensitive to pressure. Conversely, $Fe_{8.0}$ increases and $Si_{8.0}$ decreases with increasing pressure of intersection of the peridotite solidus. However, $Si_{8.0}$ may also increase with extent of melting and thus the use of this parameter is probably less reliable than FeO (Klein and Langmuir, 1989). The broad positive correlation between FeO* and $Na_{8.0}$* for some of the areas under consideration here (e.g. Seal Nunataks; Fig. 6*a*) is consistent with increasing extent of melting with decreasing pressure of peridotite solidus intersection within a single melting column, as predicted by Klein and Langmuir (1989); that is to say, the correlation reflects 'intra-column' effects. Similarly, the negative correlation between $Na_{8.0}$* and $Si_{8.0}$ also reflects intra-column effects for each group of data.

However, if averages for each region are taken (Fig. 6*a*), the basalts from dredge site 138 have significantly lower average FeO* (6.9%) than any other area, but with $Na_{8.0}$* (3.49%) within the range of the total data set. The Brabant Island basalts (FeO* 7.9–8.2%) fall in a position intermediate between the dredge samples and the remaining data and exhibit a broad range of $Na_{8.0}$* (3.2–4.1%). For areas in the range 10–10.6% FeO*, there is a considerable range in extents of melting ($Na_{8.0}$* 3.2–4.6%). If these averaged data are considered to reflect the inter-column effects described by Klein and Langmuir (1989), then the most likely origin for these basalts is by small, but variable, extents of melting at varying mean pressures; the dredge site 138 basalts represent the lowest mean pressures and most restricted range of extents of melting, and the data in the range

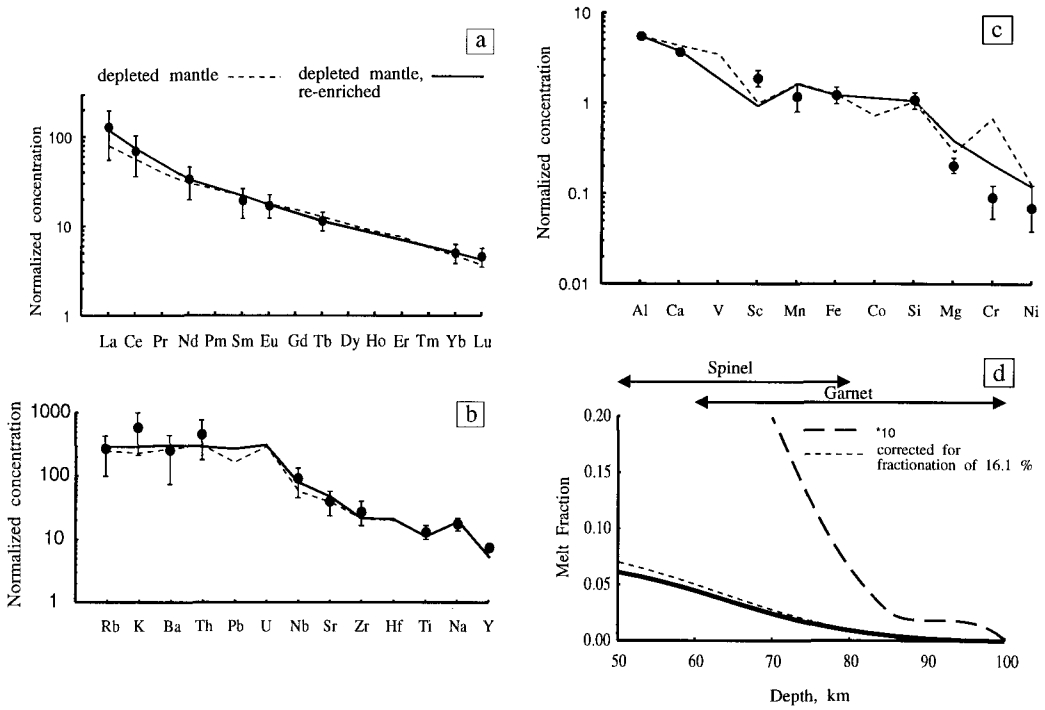

FIG. 8. Results of inversion modelling on the Antarctic Peninsula basalts following the method of McKenzie and O'Nions (1991; 1995). Note the extremely good fit of (*a*) *REE* (*b*) other incompatible elements and (*c*) major and transition elements for re-enriched depleted mantle. Dots are mean observed elemental concentrations with range. (*d*) Depth and extent of melting from *REE* inversion. Note that initial melting occurred in the garnet stability field of the mantle. See text for details of inversion modelling and Table 1 for major element data.

10.0–10.6% FeO* represent highly variable extents of melting at restricted, but high, mean pressure. Correlations between $Si_{8.0}$ and $Na_{8.0}$* are more complex. The relative positions of the data in terms of mean pressures are different from those predicted by the $Na_{8.0}$*–FeO* plot. However, because of the complicated behaviour of SiO_2 during melting and subsequent fractional crystallization (see Klein and Langmuir, 1989), we are not as confident that $Si_{8.0}$ is as good an indicator of pressures of melting as FeO*.

Absolute pressures of melting are best assessed by comparison with experimental data. Figure 7 is a plot of FeO *vs.* MgO (cation mole %) for all basalts from the Antarctic Peninsula with >8.50 MgO wt.% in order to minimize the effects of olivine fractionation (Klein and Langmuir, 1987). At these concentrations of MgO, the fractional crystallization trajectory for olivine crystallization is sub-vertical. Also plotted are experimentally determined melting relations for pyrolite at 15, 10 and 5 kbar. The dredge site 138 basalts plot directly below the 5 kbar (*c.* 16 km) melting interval, Brabant Island between the 5 and 10 kbar intervals, whereas all other remaining data sets cannot be separated and plot below a region representing $\geqslant$15 kbar (*c.* 48 km). This is generally consistent with the calculated polybaric melting trajectories of Klein and Langmuir (1989) which are illustrated as hatched lines in Fig. 6*a*. The dredge site 138 data fall on the extrapolation of the polybaric melting curve for an initial pressure of intersection of the solidus (P_0) of *c.* 15 kbar, and would require melt integration to *c.* 5 kbar, whereas the remaining samples fall between the curves for P_0 = 15 and 40 kbar, and would require melt integration to a pressure of *c.* 10–15 kbar.

In summary, unaveraged data from individual geographical localities exhibit evidence of increasing extent of melting with decreasing pressure, as predicted for intra-column variations associated with MORB (Klein and Langmuir, 1987, 1989). Inter-column effects using regionally-averaged data suggest that the trench proximal dredge site 138 basalts were generated at the lowest mean pressures in the area, the Brabant Island basalts at slightly

higher pressures, but the vast majority of the basalts were generated over a limited range of mean pressures, with integration to $\geqslant$ 15 kbar, but they represent a broad range of extents of melting which are less than those for MORB.

REE inversion modelling

An assessment of the behaviour of trace elements during mantle melting may be gained from *REE* inversion following the modelling of McKenzie and O'Nions (1991, 1995). For the purposes of inversion modelling, an average composition representing 43 basalts from Seal Nunataks and N and S Alexander Island was calculated. The *REE* data for basalts from dredge site 138 and Brabant Island were not included in the average; insufficient samples are available for rigorous mathematical manipulation. Thus, the results of this modelling are applicable to the potentially highest pressure melts in the region. The paramaterization, and the details of the modelling, are described in McKenzie and O'Nions (1991, 1995), with the modifications described in White *et al.* (1992). A series of inversions was carried out involving, successively, primitive mantle, depleted (MORB) mantle, and depleted (MORB) mantle enriched with the addition of 2% of a 0.3% melt fraction from the MORB source. The potential temperature of the mantle was varied in steps from 1300 to 1500°C, corresponding to 'normal' and 'plume' mantle temperatures, respectively, although it is important to emphasize that the temperature only influences the inversion through its effect on the depth of the garnet-spinel transition zone. Single-stage melting of depleted (MORB) type mantle (T_p 1300°C) cannot replicate the observed *REE* patterns (Fig. 8*a*) and, whilst melting of primitive mantle can produce a good fit for the *REE* in the inversion model, the isotope data require a depleted MORB-like mantle source. This leads to a model whereby a depleted MORB source is enriched by a small-melt fraction, which gives a very good fit for the *REE* and for other elements (Fig. 8*a–c*). *REE* inversion predicts that melting is initiated at *c.* 100 km depth (*c.* 30 kbar) and ceases at 52 km (*c.* 15 kbar), the maximum melt fraction being *c.* 6.5 % (Fig. 8*d*). Higher temperatures push the melting interval to greater depths (the melting interval descending to 65–135 km and 75–145 km at T_p 1400 and 1500°C, respectively). However, for reasons given earlier, there are no *a priori* reasons why the potential temperature in these regions should be anomalously high. Furthermore, regardless of variations in T_p, *REE* inversion modelling does not allow intersection of the dry peridotite solidus in the garnet stability field of the mantle. Melting must therefore be occurring on the sub-dry solidus.

The modelled major element data given in Table 1, are also plotted in Fig. 7 and fall within the field for experimental melting of pyrolite at 15 kbar, a figure consistent with the 52 km upper-depth of melting from *REE* inversion. It is clear that both major and trace element data for these high pressure basalts are consistent with their derivation by small degrees of melting over a limited range of pressures corresponding to the higher end of the range for MORB. The *REE* inversion suggests depths of initiation of melting (P_0 of Klein and Langmuir, 1987) of *c.* 30 kbar (100 km) and final depths of segregation (P_f of Klein and Langmuir, 1987) of *c.* 15kbar (52 km). In addition, MgO–FeO correlations (Fig. 7) suggest pressures of melt generation $\geqslant$15 kbar, and $Na_{8.0}$*–FeO* correlations support the notion that the basalts seen at the surface are integrated melts, with the initiation of melting occurring between 40 and 15 kbar (Fig. 6*a*). Major element and *REE* inversion modelling thus seem to be consistent both in terms of mean pressures of melt generation and extents of melting for these basalts.

Discussion

Truncated MORB melt columns and melt generation

Using the analogy of a MORB melting column, the mean pressure of melting P, that is, the pressure at which half the melting is occurring above and half below, and the mean extent of melting, F, can be

TABLE 1. Calculated and observed average major element composition of the Antarctic Peninsula basalts located > 250 km from the palaeo-trench. Calculated-observed/standard deviation (obs-calc/SD) must be greater than 2 for there to be a significant difference between calculated and observed compositions at the 95% confidence level (McKenzie and O'Nions, 1991)

	SiO_2	TiO_2	Al_2O_3	FeO	MnO	MgO	CaO	Na_2O	K_2O
obs	49.22±2.21	2.24±0.49	14.89±0.69	9.80±0.89	0.15±0.01	8.18±1.42	8.69±0.71	3.69±0.49	1.45±0.63
calc	46.07±0.81	1.87±0.24	14.14±0.93	9.37±0.97	0.20±0.05	15.06±1.00	8.67±1.07	3.82±0.29	
(obs–calc)/sd	0.19	0.53	0.06	0.003	−1.26	−4.63	−0.34	−0.35	

calculated following the method of Klein and Langmuir (1987, 1989);

$$P = P_0 - 0.707 * (P_0 - P_f) \quad ()2)$$

and

$$F = 0.006 * (P_0 - P_f) \quad (3)$$

Using the results of *REE* inversion on the potentially highest pressure melts (see also Fig. 7) to constrain the initial and final depths of melt generation, gives P_0 = 30 kbar and P_f = *c.* 15 kb, yielding P = 19 kbar and F = 9%, suggesting that all the Antarctic Peninsula basalts, with the exception of the dredge and Brabant Island samples, could have been generated from a MORB-like melting column truncated by a lithospheric cap of ~52 km thickness. Global major element correlations for MORB support an hypothesis that the lowest extents of melting are associated with the shallowest ocean ridges and lowest mean pressures of melt generation, and thus with the 'shortest' melt columns. Consequently, regionally-averaged MORB data exhibit a negative correlation between $Fe_{8.0}$ and $Na_{8.0}$, and a positive correlation between $Si_{8.0}$ and $Na_{8.0}$. These regionally-averaged data require that the mantle solidus be intersected at progressively lower mean pressures, such that the mean extent of melting decreases with decreasing pressure. Thus, for a MORB melting column with P_0 = 40 kbar, the mean pressure of melting, P, = 16 kbar and the mean extent of melting, F, = 19%, whilst a melt column with P_0 = 30 kbar, P = 11 kbar and F = 16% (Klein and Langmuir, 1987). Note that with decreasing P_0, both P and F decrease. Taking the mean major element concentrations for individual MORB melt columns yields the trend for global systematics (inter-column effects of Klein and Langmuir, 1989), which is essentially orthogonal to that of the intra-column effects. This situation is illustrated in Fig. 9. Global correlations are defined as the major element concentration at the point of intersection of the same value of F for differing P_0, which define a negative trend for FeO versus Na_2O and a positive trend for SiO_2 versus Na_2O (Fig. 9*a,b*). The major control on the pressure of generation of MORB is thus the depth of initiation of melting, P_0, as variations in the upper-limit of melt generation (P_f) are relatively minor compared to those for initial intersection of the peridotite solidus.

If a MORB melting column was truncated by a lithospheric cap, as may be the case for the Antarctic Peninsula basalts, then the thickness of the lithospheric cap becomes the most important influence on major element geochemistry. For example, for a lithospheric cap c. 50 km thick there is an overall increase in P and decrease in F for a given P_0, compared with MORB melting columns with the

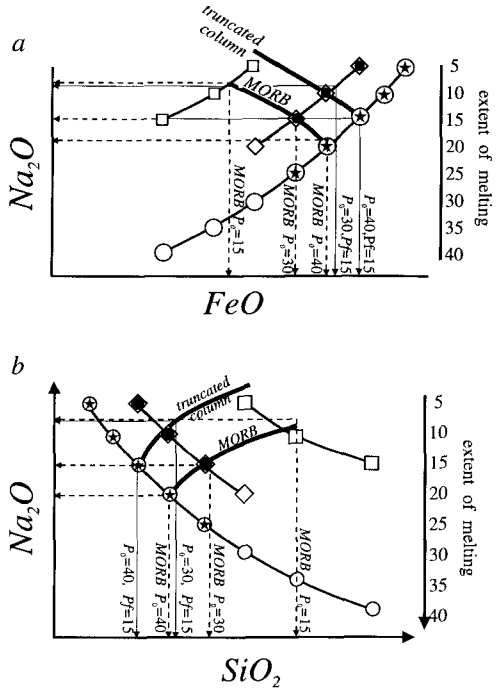

FIG. 9. Diagrammatic representation of intra- and inter-column effects on $Fe_{8.0}$, $Na_{8.0}$, and $Si_{8.0}$ for differing P_0 (circles P_0 = 40 kbar, diamonds P_0 = 30 kbar, squares P_0 = 15 kbar) for instantaneous melts from MORB melting columns (Klein and Langmuir, 1987, 1989), and their truncated equivalents for P_0 = 40 kbar, P_f = 15 kbar (stars) and P_0 = 30 kbar, P_f = 15 kbar (dots). The global MORB correlation (shaded line, labelled *MORB*) is defined by the fractionation-corrected major element composition at the intersection of F from the three melting columns. The 'global correlation' for the truncated columns is again the fractionation-corrected major element composition at the point of intersection of F for each column. Note that the trend for truncated columns has a higher Fe and lower silica content for a given Na content than MORB.

same P_0. Consequently, regionally averaged, or inter-column effects, should show evidence of higher P for a given F than the global correlations for MORB. In Fig. 9, inter-column effects for truncated melting columns again show negative correlations between FeO and Na_2O and positive correlations between SiO_2 versus Na_2O, again defined by the major element concentration at the point of intersection of F for differing P_0. However, because P is higher and F is lower than for a MORB melting column, trends for truncated columns have similar Na_2O, higher FeO* and lower SiO_2 than the global correlation for

MORB. MgO-FeO correlations (Fig. 7) suggest pressures of melting generation of $\geqslant$ 15 kb. Klein and Langmuir (1987) inferred that pressures obtained from Fig. 7 are equivalent to mean pressures of melting (P) for a MORB column. However, if we are dealing here with a truncated column, these pressures are more likely to reflect the minimum depth of melt integration, because no melting can occur at lower pressures than the base of the lithospheric cap. Indeed, the major element composition gained from *REE* inversion modelling, falls within the field for experimental melting of pyrolite at 15 kbar in Fig. 7. In this case, P will be greater than the lowest pressures of melt integration.

Effects of varying thickness of the lithospheric cap on basalt geochemistry.

Figure 10 is a plot of fractionation corrected iron concentrations in MORB (or FeO* for alkalic basalts) *vs.* fractionation corrected $Fe/Na_{8.0}$ ratio. Variations in either pressure or extent of melting will give straight line correlations on this diagram, whilst variations in both pressure and extent of melting produce curves. Global regionally-averaged data for MORB scatter around a curve corresponding to increasing extent of melting with increasing pressure, as described by Klein and Langmuir (1987, 1989). The Antarctic Peninsula data scatter around a straight line corresponding to large variations in pressure, and small but variable extents of melting compared to MORB. Additionally, it is noticeable that plume associated MORB scatter around a straight line rather than a curve and are offset to higher Fe/Na ratios than the Antarctic Peninsula basalts.

The basalts from dredge site 138, and the upper lavas from Brabant Island fall close to the composition of MORB formed by small extents of melting at low mean pressures. Dredge site 138 is <40 km on the continental side of the palaeo-trench (Hole and Larter, 1993). Assuming a slab dip of 30° the continental lithosphere is unlikely to be more than 25 km thick in this region (Hole and Larter, 1993), equivalent to a pressure of $\approx$ 8 kb. FeO and MgO data (Fig. 7) suggest a minimum pressure of 5 kbar for the generation of these basalts, equivalent to $\approx$ 16 km. For a lithospheric cap of 5 kbar acting on a MORB melting column of P_0 = 30 kbar, gives P = 12 kbar and F = 15%. These values are within the range for those expected for 'normal' i.e. non-truncated

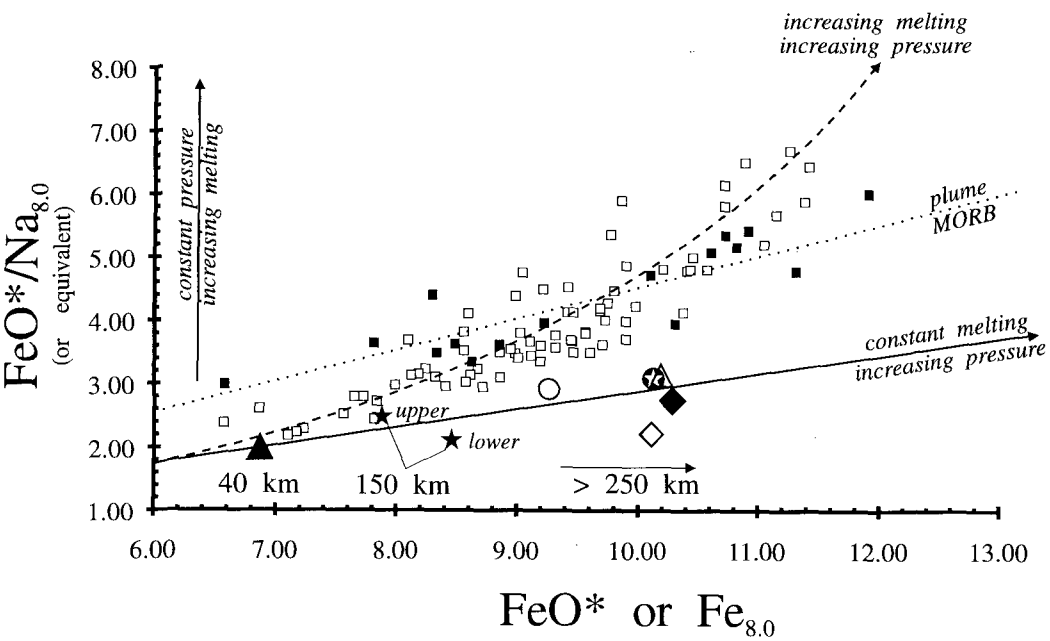

FIG. 10. Observed correlation between Fe content ($Fe_{8.0}$ for MORB and FeO* for slab window-related basalts) and fractionation corrected Fe/Na ratios. The curve for MORB (actual data shown as open squares) was calculated for $Na_{8.0}$ varying from 1.5 to 3.5% and $Fe_{8.0}$ varying from 12 to 6%, equivalent to 40 kbar and 15 kbar melting columns respectively. Plume associated MORB (filled squares; data from Klein and Langmuir (1987) and White *et al.* (1992)). Also shown is the distance from the palaeo-trench (estimated from the 2000 m bathymetric contour) of the Antarctic Peninsula basalts. Other symbols as for Fig. 6.

MORB melting columns with P_0 of 30 kbar. Consequently there is no offset to higher mean pressures of melt generation for a given extent of melting for the dredge 138 samples compared to MORB; in essence, the effect of the lithospheric cap in this region appears to be similar to that of the truncation by oceanic lithosphere for a normal MORB melting column. However, the dredge 138 samples fall on the array for MORB samples with the lowest $Fe_{8.0}$, equivalent to the shallowest intersection of the peridotite solidus ($\approx$ 15 kbar). Truncation of a 15 kbar melt column by a lithospheric cap of 5 kbar gives estimates of P = 8 kbar and F = 6.0% with melting occurring exclusively in the spinel stability field of the mantle. The half spreading rate prior to ridge crest-trench collision at this location was 20 mm yr^{-1} (Barker, 1982). Such a spreading rate would correlate with an axial crustal thickness of $\approx$ 6 km, (White *et al.*, 1992; Morgan and Chen, 1993), which equates with P_0 of $\leqslant$20 kbar according to Klein and Langmuir (1987), a figure which is in the same order as that calculated above. These values are again in the range of melt generation parameters for MORB.

The minimum depth of melt integration for the Brabant Island basalts is > 5 but < 10 kbar (Fig. 7). Assuming P_0 = 15 kbar and P_f = 7.5 kbar, yields P = 10 kbar and F = 4.5%. These estimates are consistent with the trace element data presented in Figs 2 and 6 and the general model whereby small but variable extents of melting occur at progressively increasing mean pressures. It is noticeable, however, that the mean extent of melting is less than that for Seal Nunataks for both the dredge 138 and Brabant Island samples. Nevertheless, the dredge 138 samples have MORB-normalized trace element profiles within the range for their higher pressure equivalents at Seal Nunataks. At these very low extents of melting, the trace element profiles for melting of spinel and garnet lherzolite are difficult to distinguish (Fitton and Dunlop, 1985). The most primitive dredge 138 samples have La_n/Yb_n and Sc/Yb ratios (the latter of which is a sensitive indicator of the presence of residual garnet as $k_D Sc^{gt} \gg k_D Yb^{gt}$) of 5.5 and 20 respectively (Hole and Larter, 1993; Hole *et al.*, 1995). The Sc/Yb ratios for MORB are 13–21 (mid-Atlantic ridge; Wood *et al.*, 1978). The trace element compositions of the Brabant Island samples are complicated by plagioclase accumulation (see the positive Sr spike in Fig. 1), but La_n/Yb_n ratios are 1.7–2.4 and Sc/Yb ratios are in the range 11–17. Basalts from Seal Nunataks, for a range of La_n/Yb_n 7.4–11.4 have relatively consistent Sc/Yb ratios (12.6–15.7) which are essentially buffered by the presence of residual garnet in the source. Thus the likelihood of the dredge 138 and Brabant Island samples being generated in the spinel field, and other, more easterly samples in the garnet field of the mantle, is high. This overall model would thus require increasing initial intersection of the peridotite solidus with increasing thickness of the continental lithosphere.

There is a striking relationship between distance from the palaeo-trench and FeO* content for the Antarctic Peninsula (Fig. 10). This is consistent with the truncation of a MORB melting column with a progressively thickening lithospheric cap up to a maximum of 15 kbar (*c.* 50 km), the value of *Pf* obtained form *REE* inversion modelling, and that suggested from Fig. 7 for the minimum pressure of melt integration from experimental constraints. However, during the formation of a slab window, the depth from which potential upwelling to fill the incipient void can occur depends on slab dip and distance from the trench. Thus, in trench proximal locations, there is no potential for pristine, sub-slab asthenosphere to rise above the base of the oceanic lithosphere (Hole and Larter, 1993). Consequently, intersection of the peridotite solidus is essentially constrained by distance from the trench. For a uniform slab dip of 30°, the depth to the top of the slab at 250 km from the trench would be *c.* 145 km. Thus, it is only at this distance that upwelling from depths within the garnet stability field of the mantle could occur. Consequently, the small extents of melting at high mean pressures are only recorded at 200 to 250 km from the palaeo-trench.

Generation of small melt-fractions with volatiles on the solidus: the MORB connection

Despite the overall consistency of *REE* inversion modelling and major element constraints on the pressures and extents of melting of these basalts, a significant problem remains as to their generation; in short, the mantle adiabat for T_p 1300°C does not intersect the dry peridotite solidus for mantle with a normal potential temperature until *c.* 15 kbar, which is the inferred upper pressure limit of segregation for the high-pressure basalts in this region. For reasons stated earlier, and using the results of *REE* inversion, there is no reason to suppose that the mantle in this region is unusually hot; even if the potential temperature is increased to 1500°C, the melting interval is forced to deeper levels, and still no intersection of the dry peridotite solidus can occur. Thus, melting must be occurring on the sub-dry solidus. Indeed, the temperature estimates produced by Klein and Langmuir (1987) for varying P_0, rely on the temperature of intersection of the dry solidus at P_0; the possibility for melt production on the volatile-bearing solidus was not addressed, and there is no *a priori* reason why MORB-source mantle should have significantly higher T_p locally, except near to hotspots. Furthermore, the subduction of a spreading

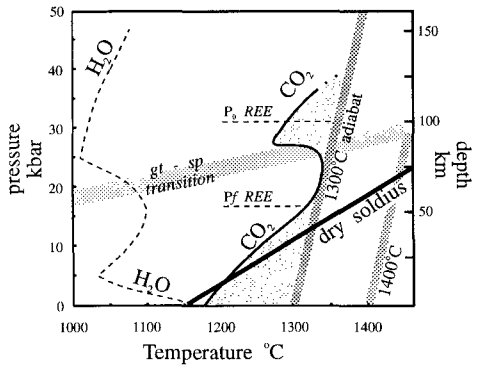

FIG. 11. *P–T* diagram showing the position of the dry, H_2O- and CO_2-saturated peridotite solidi, relative to the 1300°C T_p adiabat. Pecked lines labelled P_0 *REE* and P*f REE* are the depths of initial and final melting taken from *REE* inversion of the Antarctic Peninsula basalts. Peridotite solidi from Wyllie (1982, 1987), Olafsson and Eggler (1993), Thompson (1992) and McKenzie and Bickle (1988).

ridge will not increase T_p in the adiabatic part of the wedge, but will merely heat up the overlying lithosphere. Therefore, if elevated mantle temperatures, or localized crustal extension are not responsible for the formation of slab window-related basalts, it is necessary to invoke hydration or carbonation of the mantle to reduce the solidus temperatures (Fig. 11).

Hydration of the mantle wedge during 'normal' subduction appears to be required to generate the volumes of melts — often strongly quartz normative — emplaced in the arc environment. The H_2O/CO_2 ratios of such melts are often high (Gill, 1981) but data are scarce. Nonetheless the observations are broadly consistent with the experimental data (Wyllie, 1982,1987) The lavas erupted in the post-subduction, slab window environment are predominantly (but not exclusively) nepheline-normative, similar to ocean island basalts. This is consistent with melting under lower H_2O/CO_2 conditions (Wendlandt and Mysen, 1980; Wyllie, 1987) The presence of CO_2 reduces the solidus temperature of mantle peridotite (Fig. 11) and also pushes the eutectic to increasingly undersaturated conditions (Wyllie, 1982, 1987). The low activity of water, in turn, is consistent with the trace element data which show an absence of a slab-derived component.

The model we propose is that the post-subduction magmas are generated by a multi-stage process, beginning with small-degree carbonated and hydrous melting of the sub-slab mantle (see also Hole *et al.*, 1995). Flow of sub-slab mantle into the wedge is supported by the chemical data, which preclude significant involvement of a subduction zone component. The sub-slab mantle would thus appear to be physically displacing the original mantle wedge. The *REE* inversion and major element constraints require that P_0 increases with distance from the continental margin. The *REE* inversion also requires pre-enrichment of the mantle. The reason for this is not obvious, because it would be expected that the highest pressure of melt generation should still be that of the initial intersection of the solidus beneath the abandoned spreading ridge, i.e. 20 kbar. What is important here, is the limitation on the finite depth from which upwelling to fill the slab window void can occur following passage of the slab beneath a particular location. For a slab dip of *c.* 30°, the upper surface of the slab, 250 km from the trench, will be at *c.* 140 km depth. If the thickness of the slab is *c.* 40 km then the removal of the subducting slab allows upwelling from a maximum depth of *c.* 180 km (~56 kbar). Details of the initial intersection of the CO_2-bearing solidus with the T_p 1300°C adiabat are not available, although extrapolation suggests 45–50 kbar (see Wyllie, 1987); by 30 kbar (the lower limit of melting obtained from *REE* inversion) intersection of the adiabat and CO_2-bearing solidus has occurred, and melt can be generated on the CO_2-bearing solidus, as long as upwelling has been from greater than this pressure. Therefore, any melting must initially occur at high pressure, within the garnet-stable facies. The small-degree melts will be strongly heavy-*REE* depleted and incompatible-element-enriched. As they percolate upwards the extent of melting will increase, but the CO_2 will be depleted in the source and thus the solidus temperature of the residual mantle will be driven to progressively higher temperatures. Consequently the extent of melting will be self-limiting, and must occur over a limited range of pressures corresponding to the depth of the intersection of the CO_2 saturated solidus with the adiabat, the onset of CO_2 dissolution in the first-formed melt fractions, and the base of the lithospheric cap.

This initial melting process could also occur under a normal spreading axis, without the need for elevated temperatures and intersection of the dry-peridotite solidus. Whilst most models require thermal anomalies in the mantle to initiate melting at varying depths (e.g. Klein and Langmuir, 1987, 1989; Humler *et al.*, 1993; McKenzie and O'Nions, 1991), the model here implies that all MORB could be produced at T_p 1300°C with CO_2 on the solidus. Because the largest melt fractions in a MORB column will be formed at less than the mean pressure of melting, then the trace element composition of the high pressure, sub-dry solidus early formed melts will be lost during successive integration, particularly

for melting columns where P_0 is large. Thus, whilst the initial melt-fractions from sub-dry solidus melting would compositionally differ from those generated by high temperature dry melting, the final product i.e. MORB, would still carry a signature of $P < 15$ kbar. Humler *et al.*, (1993) noted striking correlations between S-wave velocities at varying depths in the mantle and major element chemistry of MORB. They argued that the positive linear relationship between $Na_{8.0}$ and % velocity variation for all MORB in the depth region 110–130 km was a result of thermal anomalies in the mantle and not the presence of melt, whilst at 90 km, the same correlation only for slow spreading centres was the result of melt retention in the mantle. Depths of 110–130 km correspond to the region in the mantle where the model presented here predicts melting with CO_2 on the solidus. Therefore, we argue that the observed S-wave velocity variations are the result of the presence of low viscosity, low density carbonated melts in the mantle, and not a result of chemical or thermal heterogeneity.

Conclusions

All the above observations are consistent with the truncation of a MORB-like melting column by a lithospheric cap. We therefore suggest that the Antarctic Peninsula slab window-related basalts are samples of the small melt-fraction precursors to MORB tholeiites. The MORB-like isotopic and highly-incompatible element character of the alkali basalts associated with slab-windows preclude significant involvement of a subduction component, be it inherited from the slab or from the overlying asthenosphere or mechanical boundary layer. This strongly suggests to us that the small melt-fraction was not generated in the mantle wedge during subduction, and remobilized during subsequent extension or thermal relaxation. Had this been the case, we would expect a supra-subduction signature in these basalts. In some regions, this is indeed seen (e.g. southern Baja California: Rogers and Saunders, 1989), often in juxtaposition with alkalic basalts with a minor or non-existent slab signature. Displacement of the asthenosphere by sub-slab mantle with its complement of small melt-fractions, appears to be a viable model to explain this juxtaposition of compositionally and isotopically distinct melts.

If this is correct, it has some important implications for magma generation. Firstly, it lends further support to the hypotheses based on U-Th disequilibrium studies and theoretical grounds, that small melt fractions are indeed present beneath spreading axes (McKenzie, 1985*b*; McKenzie and Bickle, 1988; Beattie, 1993) with the concomitant implications for trace element fractionation; indeed, the slab window-related basalts are probably the closest erupted analogues to MORB precursor melts yet reported. Secondly, the model implies that *HREE*-depleted alkaline basalts require neither lithospheric extension, nor high mantle temperatures for their formation. Thirdly, the development of an enriched zone of mantle, particularly if it is able to stabilize in the lithosphere, will enable isotopic diversity.

The slab window environment provides unusual circumstances with which to constrain these magmatic processes. It is, as far as we are aware, one of the few environments where we can be confident that melts have undergone garnet fractionation but are not associated with a mantle plume. They thus provide very clear evidence for the role of volatiles in reducing mantle solidus temperatures, and for the role of small melt-fractions, initially formed in the garnet stability field, in generating isotopic diversity in the mantle.

Acknowledgements

MJH wishes to thank the participants at the 1994 Penrose Conference, N California, for a number of days of stimulating discussion. Financial support for attendance was provided by the NSF and the UK Transantarctic Association. Prof. Dan McKenzie and Dave Latin are thanked for their help with the *REE* inversion modelling.

References

Barker, P.F. (1982) The Cenozoic subduction history of the Pacific margin of the Antarctic Peninsula: ridge crest-trench interactions. *J. Geol. Soc. London,* **139**, 787–801.

Beattie, P. (1993) Uranium-thorium disequilibria and partitioning on melting of garnet lherzolite. *Nature*, **363**, 63–5.

Bevier, M. L. (1983) Implications of chemical and isotopic composition for petrogenesis of Chilcotin Group Basalts, British Columbia. *J. Petrol.,* **24**, 207–26.

Brodholt, J.P. and Batiza, R. (1989) Global systematics of unaveraged mid-ocean ridge basalt compositions: Comment on 'Global correlations of ocean ridge basalt chemistry with axial depth and crustal thickness' by E.M. Klein and C.H. Langmuir. *J. Geophys. Res.,* **94**, 4231–9.

Chaffey, D.J., Cliff, R.A. and Wilson, B.M. (1989) Characterization of the St Helena magma source. In *Magmatism in the ocean basins.* (A.D. Saunders and M.J. Norry, eds.) *Spec. Pub. Geol. Soc. London*, **42**, 313–45.

Chauvel, C., Hofmann, A.W. and Vidal, P. (1992) HIMU-EM: the French Polynesian connection. *Earth Planet. Sci. Lett.,* 110, 99–119.

Davies, G. R., Norry, M. J., Gerlach, D. C. and Cliff, R. A. (1989) A combined chemical and Pb-Sr-Nd study of the Azores and Cape Verde hotspots: the geodynamic implications. In *Magmatism in the ocean basins.* (A.D. Saunders and M.J. Norry, eds.) *Spec. Pub. Geol. Soc. London,* **42**, 231–56.

Dickinson, W. R. and Snyder, W. S. (1979) Geometry of subducted slabs related to the San Andreas transform. *J. Geology,* 87, 609–27.

Elliot, T. R., Hawkesworth, C. J. and Gronvold, K. (1991) Dynamic melting of the Iceland plume. *Nature,* 351, 201–6.

Fitton, J.G. and Dunlop, H.M. (1985) The Cameroon line, West Africa, and its bearing on the origin of oceanic and continental alkali basalt. *Earth Planet. Sci. Lett,.* **72,** 23–38.

Forsythe, R. D. and Nelson, E. P. (1985) Geological manifstations of ridge collision: evidence from the Golfo de Penas-Taito Basin, Southern Chile. *Tectonics*, **4**, 477–495.

Gill, J. B. (1981) *Orogenic andesites and plate tectonics.* Berlin: Springer-Verlag.

Hart, S.R. (1988) Heterogeneous mantle domains: signatures, genesis and mixing chronologies. *Earth Planet. Sci. Lett.,* **90**, 273–96.

Hole, M.J. (1988) Post-subduction alkaline volcanism along the Antarctic Peninsula. *J. Geol. Soc. London,* 145, 985–8.

Hole, M.J. (1990) Geochemical evolution of Pliocene-Recent post-subduction alkalic basalts from Seal Nunataks, Antarctic Peninsula. *J. Volcanol. Geotherm. Res.*, **40**, 149–67.

Hole, M.J. and Larter, R. D. (1993) Trench proximal volcanism following ridge crest -trench collision along the Antarctic Peninsula. *Tectonics,* 12, 897–910.

Hole, M.J., Saunders, A.D., Marriner, G.F. and Tarney, J. (1984) Subduction of pelagic sediments: implications for the origin of Ce-anomalous basalts from the Mariana islands. *J. Geol. Soc. London,* 141, 453–72.

Hole, M.J., Rogers, G., Saunders, A. D. and Storey, M. (1991) The relationship between alkalic volcanism and slab-window formation. *Geology,* 19, 657–60.

Hole, M.J., Kempton, P.D. and Millar, I.L. (1993) Trace element and isotope characteristics of small degree melts of the asthenosphere; evidence from the alkalic basalts of the Antarctic Peninsula. *Chem. Geol.,* 109, 51–68.

Hole, M.J., Saunders, A. D., Sykes, M. A. and Rogers, G. (1995) The relationship between alkalic magmatism, lithospheric extension and slab window formation along continental destructive plate margins. In *Volcanism associated with extension along consuming plate margins* (J.L. Smellie, ed.) Spec. Pub. Geol. Soc. London, **81,** 265–85.

Humler, E., Thirot, J-L. and Montagner, J-P. (1993) Global correlations of mid-ocean ridge basalt chemistry with seismic tomography images. *Nature,* **364**, 225–7.

Ito, E White, W. M. and Gopel, C. (1987) The O, Sr, Nd and Pb isotope geochemistry of MORB. *Chem. Geol.,* 62, 157–76.

Johnson, C. M. and O'Neil, J. R. (1984) Triple junction magmatism: a geochemical study of Neogene volcanic rocks in western California. *Earth Planet. Sci. Lett.,* 71, 241–62.

Klein, E. M. and Langmuir, C. H. (1987) Global correlations of ocean ridge basalt chemistry with axial depth and crustal thickness. *J. Geophys. Res.*, **92**, 8089–115.

Klein, E. M. and Langmuir, C.H. (1989) Local versus global variations in mid-ocean ridge basalt composition: a reply. *J. Geophys. Res.*, **94,** 4241–52.

Larter, R. D. and Barker, P. F. (1991) Effects of ridge-crest trench interaction on Antarctic-Phoenix spreading: forces on a young subducting plate. *J. Geophys. Res.*, **96** , 9583–607.

LeMasurier, W. E. and Thomson, J. W. (1990) *Volcanoes of the Antarctic Plate and Southern Oceans.* American Geophysical Union, Antarctic Research Series, **48**, 147–256.

McKenzie, D.P. (1984) The generation and compaction of partially molten rock. *J. Petrol.*, **25**, 713–65.

McKenzie, D.P. (1985*a*) The extraction of magma from the crust and mantle. *Earth Planet. Sci. Lett.,* 74, 81–91.

McKenzie, D.P. (1985*b*) ^{230}Th-^{238}U disequlibrium and the melting processes beneath ridge axes. *Earth Planet. Sci. Lett.,* 72, 149–57.

McKenzie, D.P. and Bickle, M. J. (1988) The volume and composition of melt generated by extension of the lithosphere. *J. Petrol.,* 29, 625–79.

McKenzie, D.P. and O'Nions, R.K. (1991) Partial melting distributions from inversion of Rare Earth Element concentrations. *J. Petrol.,* **32**, 1021–91.

McKenzie, D.P. and O'Nions, R.K (1995) The source regions of ocean island basalts. *J. Petrol.*, **36**, 133–59.

Morgan, J.P., and Chen, Y.J. (1993) Dependence of ridge-axis morphology on magma supply and spreading rate. *Nature*, **364**, 706–8.

Olafsson, M. and Eggler, D.H. (1983) Phase relations of amphibole, amphibole-carbonate and phlogopite-carbonate peridotite: petrologic constraints on the asthenosphere. *Earth. Planet. Sci. Lett.,* 64, 305–15.

Oxburgh, E.R. (1980) Heat flow and magmagenesis. In *Physics of Magmatic Processes* (R.B. Hargraves, ed.) New Jersey: Princeton Univ. Press, 161–99.

Palacz, Z. A. and Saunders, A. D. (1986) Coupled trace element isotope enrichment in the Cook-Austral-Samoa islands, southwest Pacific. *Earth. Planet. Sci. Lett.*, **79**, 270–80.

Pearce, J.A. (1983) Role of the sub-continental lithosphere in magma genesis at active continental

margins. In *Continental Basalts and Mantle Xenoliths*. (C.J. Hawkesworth and M.J. Norry, eds.) Nantwich, England: Shiva Publishing, pp. 230–49.

Ringe, M. J. (1991) Volcanism on Brabant Island, Antarctica. In *The geological evolution of Antarctica* (M.R.A. Thomson, J.A. Crame and J.W. Thomson, eds.) Cambridge, England: Cambridge University Press, 515–9.

Rogers, G. and Saunders, A. D. (1989) Magnesian Andesites from Mexico, Chile and the Aleutian Islands: implications for magmatism associated with ridge-trench collisions. In *Bonninites and related rocks* (A.J. Crawford, ed.) London: Unwin-Hyman, 416–45.

Saunders, A. D., Rogers, G., Marriner, G. F., Terrell, D. J. and Verma, S. P. (1987) Geochemistry of Cenozoic volcanic rocks, Baja California, Mexico: implications for the petrogenesis of post-subduction magmas. *J. Volcanol. Geotherm. Res.*, **32**, 223–45.

Saunders, A. D., Norry, M. J. and Tarney, J. (1988) Origin of MORB and chemically depleted mantle reservoirs: trace element constraints. *J. Petrol. Special Lithosphere Issue*, 414–45.

Smellie, J.L., Pankhurst, R.J., Hole, M.J.and Thomsom, J.W. (1988) Age, distribution and eruptive conditions of late Cenozoic alkaline volcanism in the Antarctic Peninsula in eastern Ellsworth Land: Review. *British Antarctic Survey Bull.*, **80**, 21–49.

Storey, M., Rogers, G., Saunders, A. D. and Terrell, D., (1989) San Quintín volcanic field, Baja California, Mexico: within-plate magmatism following ridge subduction. *Terra Nova*, **1**, 195–202.

Sun, S-S. and McDonough, W. F. (1989) Chemical and isotopic systematics of oceanic basalts: implications for mantle composition and processes. In *Magmatism in the ocean basins* (A.D. Saunders and M.J. Norry, eds.) Spec. Pub. Geol. Soc. London, **42**, 313–45.

Thompson, A.B. (1992) Water in the Earth's mantle. *Nature*, **358**, 295–302.

Thorkelson, D. J. and Taylor, R. P. (1989) Cordilleran slab windows. *Geology*, **17**, 833–6.

Weaver, B. L. (1991) The origin of ocean island basalt end-member compositions: trace element and isotopic constraints. *Earth Planet. Sci. Lett.*, 382–97.

Wendlandt, R.F. and Mysen, B.O. (1980) Melting phase relations of natural peridotite + CO_2 as a function of melting at 15 and 30 kbar. *Amer. Mineral.*, **65**, 37–44.

White R.S., McKenzie, D.P. and O'Nions, R.K. (1992) Oceanic crustal thickness from seismic measurements and rare earth element inversions. *J. Geophys. Res.*, **97**, 683–716.

Wood, D. A., Varet, J., Bougault, H., Corre, O., Joron, J-L., Trueil, M., Bizouard, H., Norry, M. J., Hawkesworth, C. J. and Roddick, J. C. (1978) Transition metal and trace element analyses of Leg 49 samples. *Init. Rep. Deep Sea Drill. Proj.*, **49**, 897–902.

Wyllie, P.J. (1982) Subduction products according to experimental predictions. *Bull. Geol. Soc. America*, **93**, 468–76.

Wyllie, P.J. (1987) Discussion on recent papers on carbonated peridotite, bearing on mantle metasomatism and magmatism. *Earth Planet. Sci. Lett.*, **82**, 391–7.

[*Revised manuscript received 10 July 1995*]